



ELSEVIER

Contents lists available at ScienceDirect

Inorganica Chimica Acta

journal homepage: www.elsevier.com/locate/ica

Research paper

Effective transesterification of triglyceride with sulphonated modified SBA-15 (SBA-15-SO₃H): Screening, process and mechanism

Ningmeng Hu^a, Zhaoni Kong^a, Liang He^b, Ping Ning^a, Junjie Gu^a, Rongrong Miao^a, Xiangqian Sun^c, Qingqing Guan^{a,*}, Peigao Duan^{d,*}

^a Faculty of Environmental Science and Engineering, Kunming University of Science and Technology, Kunming 650500, China

^b Faculty of Chemical Engineering, Kunming University of Science and Technology, Kunming 650500, China

^c Faculty of Energy & Environment Science, Yunnan Normal University, Kunming 650500, China

^d Department of Applied Chemistry, Henan Polytechnic University, Jiaozuo 454003, China

ARTICLE INFO

Keywords:

Biodiesel

Transesterification

Triglyceride

SBA-15-SO₃H

ABSTRACT

Different morphologies of ZrO₂ were produced by different templates: ZrO₂(CaCO₃), ZrO₂(C₁₂H₂₅SO₃Na), ZrO₂(C₁₂H₂₅SO₄Na), ZrO₂(CTAB), and solid superacids, such as ZrO₂/SBA-15, SO₄²⁻/ZrO₂, SO₄²⁻/ZrO₂/SBA-15, and SBA-15-SO₃H. The catalytic transesterification activities of these catalysts were tested. The more highly acidic catalysts and higher surface areas led to higher catalytic activity. In particular, the conversion yield of triglyceride reached 90.1% and was maintained for 90 min at 200 °C with 5.0 wt% SBA-15-SO₃H, indicating this material to be one of most effective acid catalysts for the transesterification process. The mechanism indicated that the most important process was the abstraction of hydrogen from alcohols and α -substituted carboxylic glycerides. In the initial transesterification, the alcohol hydrogen atoms could be attracted onto the surface. Then, the nucleophilic attack of the alcohol led to the α -substituted carboxylic glyceride. Finally, mono-glycerides, diglycerides or glycerine were released from the surface by proton (H⁺) replacement.

1. Introduction

The declining availability of fossil energy and increased global warming drive the exploration of alternative energy sources. Biomass energy, which is renewable, sustainable and environmentally friendly, has gained tremendous attention [1,2]. Biodiesel, which is normally obtained from some animal fats and plant raw materials, has been widely investigated and is already being used in commercial applications [3,4]. In 2016, the US had a biodiesel production capacity of 2.6 billion litres. Currently, transesterification is regarded as the best method for producing higher quality biodiesel. However, transesterification reactions will proceed either slowly or not at all under normal conditions. Thus, improvements to the production process of biodiesel play an important role in this field [5].

Many researchers have tried to enhance the efficiency of biodiesel production through the use of catalysts, such as enzymes [6], alkalis [7] and acids [8]. Although using enzyme catalysts has some advantages, it also suffers from high costs, large reaction volumes and slow reaction rates [9,10]. Base catalysis is economical and requires low temperatures and pressures, but the alkaline catalyst will react with the free fatty acids to form soaps when the raw materials (oils or fats) have a high

percentage of water or free fatty acids. Some researchers have tried to use heterogeneous base catalysts; for instance, Lei et al. [11] showed that an 87.0% conversion of methyl stearate was achieved at 120 °C for 4 h over MgAl layered double hydroxide. Kouzu et al. [5] reported a yield of 89% for the transesterification of waste cooking oil with a CaO heterogeneous base catalyst. Even heterogeneous base catalysts still react with the free fatty acids to form soaps, though, so it is difficult to separate the products [12].

Acid catalysis is more suitable in this situation than is base catalysis [13]. Unfortunately, some mineral acids, such as H₂SO₄, are highly corrosive [14]. To avoid the corrosion problems caused by mineral acids, reusable, non-corrosive and easily removable heterogeneous solid acid catalysts are a good choice, which can be easily recycled and give rise to minimal corrosion. Therefore, solid catalysts are often employed in transesterification reactions [15].

Previously, we reported transesterification by Lewis acid AlCl₃ catalysis in ethanol and carbon dioxide as cosolvents and by a high-performing sulphonated multi-walled carbon nanotube (S-MWCNT) [16,17]. In this work, we performed a further screening of different catalysts. Additionally, some research has shown that mesoporous silica, such as SBA-15 and mesoporous silica (OMS), has a tuneable pore

* Corresponding authors.

E-mail addresses: 15545488@qq.com (Q. Guan), pgduan@hpu.edu.cn (P. Duan).

<https://doi.org/10.1016/j.ica.2018.07.032>

Received 26 April 2018; Received in revised form 21 July 2018; Accepted 21 July 2018

Available online 25 July 2018

0020-1693/ © 2018 Elsevier B.V. All rights reserved.

structure, high surface area and tailored composition, which may be applied to adsorb compounds, separate gases and perform catalysis [18,19]. Specifically, the morphology of SBA-15 can be tailored according to the given requirements [20–22], and the independent outer particle surface and inner pore surfaces can also be functionalized [5,23]. SBA-15 might enhance the catalytic activity of the transesterification when acid-functionalized [24,25].

Herein, this work screened and compared different solid acid catalysts under identical conditions. In particular, an efficient solid-acid catalyst, SBA-15-SO₃H, was further studied for the transesterification of trilaurin in ethanol at temperatures of 160, 180, 200 and 230 °C. The textural properties of SBA-15-SO₃H were characterized by BET, XRD, SEM, TEM, XPS, FT-IR and Py-FTIR. The yields of each conversion process were analysed by high-performance liquid chromatography (HPLC). Additionally, the mechanism was discussed to provide an insight into the transesterification reactions of solid acid catalysts.

2. Experimental section

2.1. Materials

Triblock copolymer PEO20-PPO70-PEO20 (P123) and tetraethyl orthosilicate (TEOS) were purchased from Sigma-Aldrich. (3-Mercaptopropyl) trimethoxysilane (MPTMS, 98%) was purchased from MACKLIN. Concentrated H₂SO₄ (AR) and HCl (AR) were purchased from Chengdu Kelong Chemical Reagent Factory (China) and Tianjin Fengchuan Reagent Technologies Co. Ltd. (China), respectively. Trilaurin (98%) and ethanol (99.9%) were supplied from Aladdin. All other chemicals, including SDS, NaCl and NaOH, were analytic grade and used without any further purification.

2.2. Catalyst preparation

In this study, we choose different template methods for controlling the morphologies of ZrO₂, which has been rewritten in the section on screening the catalyst. We chose different templates and methods to prepare ZrO₂, including, for example, ZrO₂(CaCO₃), which used CaCO₃ cubes as templates to prepare novel ZrO₂ hollow microboxes [26]. ZrO₂(SDS) was prepared by a lamellar liquid crystal template method, using sodium dodecyl sulphate as the template to produce compounded cubic phase spherical zirconia nanopowder [27].

The catalysts were synthesized using P123 as the template, TEOS as the main silicon source, and MPTMS as an additional source of silicon. The molar ratios of n(P123)/n(TEOS)/n(MPTMS)/n(HCl)/n(H₂O) = 7 × 10⁻⁴/x/0.004/0.24/6.67, where x represents the molar amount of TEOS. First, 8 g P123 was dissolved in 195.16 ± 0.01 g deionized water at room temperature, and the solution was stirred for 2 h. Then, 50.05 ± 0.01 g concentrated hydrochloric acid was added and stirred for 30 min. Afterwards, 15.35 ± 0.01 g tetraethyl orthosilicate was added and stirred for 45 min, and then, 1.607 ± 0.01 g MPTMS and 16.73 ± 0.01 g hydrogen peroxide were added, followed by stirring at 40 °C for 20 h. The mixture was transferred into a Teflon-lined stainless-steel autoclave, which was then sealed and maintained at 100 °C for 24 h. Lastly, the mixtures were refluxed with 400 mL hydrochloric acid/ethanol solution (volume ratio 2/100) for 12 h to remove the template P123. The resulting solid products were dried at 80 °C for 8 h to obtain the SBA-15-SO₃H.

2.3. Characterization of SBA-15-SO₃H catalysts

The N₂ adsorption-desorption isotherms were measured at liquid nitrogen temperature, -196 °C, on a Micromeritics Tristar 3020 analyser, from which the specific surface area, pore volume and average pore diameter were calculated by applying multiple-point Brunauer-Emmett-Teller (BET) and Barrett-Joyner-Halenda (BJH) models on adsorption branches. XRD measurements were collected on a Bruker D8

Advance X-ray diffractometer, using Cu Kα radiation (k = 1.5404 Å) at 40 kV and 20 mA in the 2θ range of 0.5–6.0°. Scanning electron microscopy (SEM) images of the samples were recorded on a QUANTA F250 microscope. Transmission electron microscopy (TEM) was obtained using a Tecnai G2 20 microscope operated at 100 kV. The sulfonation degree of SBA-15 was determined by X-ray photoelectron spectroscopy (XPS). FTIR was recorded on a Nicolet iS50 FTIR spectrometer equipped with a smart collector using pressed KBr powder discs.

2.4. Experimental process

The experimental device has been described in detail in our previous work [16]. Transesterification reactions were performed with triacylglycerol and liquid ethanol with a mass ratio of 1:10. The SBA-15-SO₃H catalyst with 5.0 wt% loading was placed in the 4-mL reactor, which was vertically positioned in a Techne fluidized sand bath (model SBL-2). In addition, different kinds of catalysts were used, and then, the best was selected as the core catalyst in this study. The transesterification reaction was carried out at a series of temperatures, i.e., 160, 180, 200 and 230 °C, with a series of times of 15, 30, 45, 60, 75 or 90 min. The vessels were removed from the sand bath and cooled to room temperature. At last, the products were washed with methanol at least three times so that all products were recovered.

The products were analysed by HPLC equipped with an AcclaimTM C18 column (4.6 mm i.d. × 250 mm length). HPLC was conducted using a mobile phase of 65% methanol and 35% acetonitrile at a flow rate of 0.8 mL/min for 25 min. The UV detector was set at 210 nm, and the column temperature was 35.0 °C.

3. Results and discussion

3.1. Screening of transesterifications by triglyceride catalysts

The experiments to screen and compare with different catalysts used the transesterification of triglycerides with ethanol as a model reaction. The different morphologies of ZrO₂ produced by different templates, including ZrO₂(CaCO₃), ZrO₂(C₁₂H₂₅SO₃Na), ZrO₂(C₁₂H₂₅SO₄Na), ZrO₂(CTAB) and solid superacids, such as ZrO₂/SBA-15, SO₄²⁻/ZrO₂, SO₄²⁻/ZrO₂/SBA-15 and SBA-15-SO₃H, were tested. A blank reaction was also conducted to make a comparison. The reaction time and temperature were fixed at 60 min and 200 °C, respectively.

The efficiencies for the transesterification of triglyceride are shown in Table 1. The triglyceride conversion rate of the blank experiment is very low, but when the catalysts are introduced, the triglyceride conversion rates increase significantly, indicating that the catalysts all possess some catalytic activity for the transesterification of triglycerides. However, the activity of different catalysts varies greatly.

Table 1
Physicochemical properties and comparison of yield of different catalysts.

Sample	Surface area (m ² /g)	Pore volume (cm ³ /g)	Yield (%)
NO	0	0	1.5
ZrO ₂ (CaCO ₃)	67.02	0.286	21.7
ZrO ₂ (C ₁₂ H ₂₅ SO ₃ Na)	102.01	0.39	38.1
ZrO ₂ (C ₁₂ H ₂₅ SO ₄ Na)	88.13	0.393	27.5
ZrO ₂ (CTAB)	69.57	0.134	14.1
SO ₄ ²⁻ /ZrO ₂ [5%SO ₄ ²⁻ (H ₂ SO ₄)]	59.87	0.316	19.1
SO ₄ ²⁻ /ZrO ₂ [10%SO ₄ ²⁻ (H ₂ SO ₄)]	57.1	0.137	46.7
SO ₄ ²⁻ /ZrO ₂ [5%SO ₄ ²⁻ (NH ₄) ₂ SO ₄]	63.79	0.245	37.8
SO ₄ ²⁻ /ZrO ₂ [10%SO ₄ ²⁻ (NH ₄) ₂ SO ₄]	65.42	0.293	49.7
SBA-15	794.45	1.036	4.7
ZrO ₂ /SBA-15	567.14	0.468	57.7
SO ₄ ²⁻ /ZrO ₂ /SBA-15	260.53	0.418	54.6
SBA-15-SO ₃ H	768.48	0.891	88.1

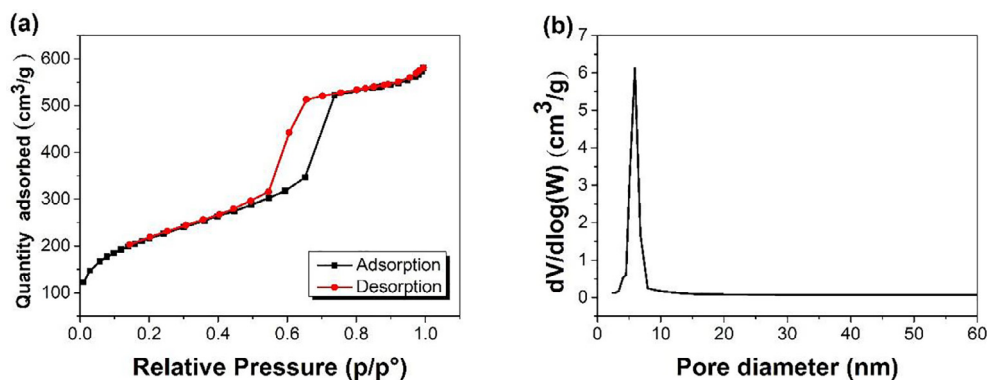


Fig. 1. N_2 adsorption-desorption isotherm of synthesized catalysts (a); pore size distributions of SBA-15- SO_3H (b).

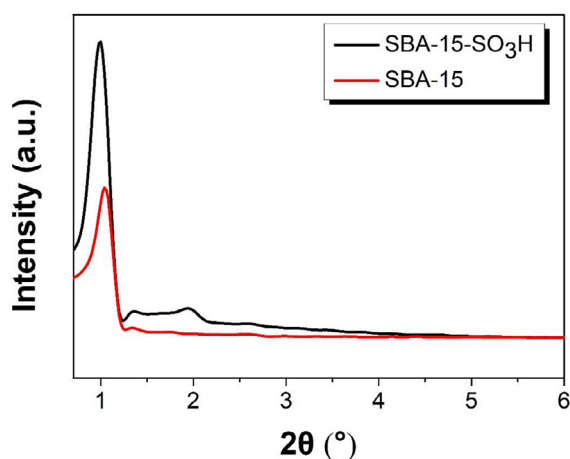


Fig. 2. Small-angle X-ray diffraction patterns for materials SBA-15 and SBA-15- SO_3H .

According to Table 1, SO_4^{2-}/ZrO_2 [5% SO_4^{2-} (NH_4) $_2SO_4$], $ZrO_2/SBA-15$ and SBA-15- SO_3H showed superior activity. These results are consistent with our previous speculation that the more highly acidic catalysts and higher surface areas lead to higher catalytic activity [16,17]. The most active material was SBA-15- SO_3H , achieving an 88.1% yield of triglyceride. As SBA-15 has no obvious activity in the transesterification reaction, the increase in efficiency by the modification of sulphonic acid to make solid superacids is obvious. Since SBA-15- SO_3H shows excellent catalytic performance compared with that of those catalysts, further research will be described in the following section.

3.2. Catalyst characterization

Fig. 1 shows the nitrogen adsorption-desorption isotherms and pore size distributions. According to IUPAC, the isotherm is a typical type IV [28]. In Fig. 1a, the isotherms with a sharp capillary condensation step in the adsorption and desorption curve, the presence of the H1 hysteresis loop indicates that the material has a uniform pore size and good connectivity, with a 2D hexagonal structure of ordered mesoporous materials [29]. The BET procedure using P/P_0 at this area of the isotherms calculated the specific surface areas; using the BJH pore analysis method yielded the pore size distribution. As seen, the average pore diameters and pore size distributions of SBA-15- SO_3H are displayed in Fig. 1b, showing a narrow pore size distribution.

Fig. 2 shows the low-angle XRD patterns obtained for SBA-15 and functionalized SBA-15- SO_3H . An intense diffraction peak at approximately $2\theta = 0.9$ – 1.0° , found in the XRD patterns, is indexed to the (100) plane, suggesting that the material was ordered in 2D $P6mm$ hexagonal mesoporous structures with a uniform mesoporous size distribution [30]. Obviously, SBA-15- SO_3H has similar XRD patterns to those of the SBA-15 support, even after the sulphonic acid groups were introduced into the SBA-15. Furthermore, the mesoporous structure was virtually retained as evidenced by the SEM and TEM (Fig. 3a–b), which show regular 2D $P6mm$ hexagonal mesoporous structures. Moreover, compared with those of pure SBA-15, the (110) and (200) diffraction peaks of the SBA-15- SO_3H materials gradually decreased, and a slight shift in the peak position to higher angles suggested the decrease in the pore size in the presence of the $-SO_3H$ groups [31]. According to these results, it was revealed that the SBA-15- SO_3H production process was successful, and the pore structure of the SBA-15 after introducing $-SO_3H$ was not damaged.

Fig. 4 shows the energy positions for the C 1s, O 1s, S 2p and Si 2s on the SBA-15- SO_3H surface. Fig. 4b reveals the existence of S in the SBA-

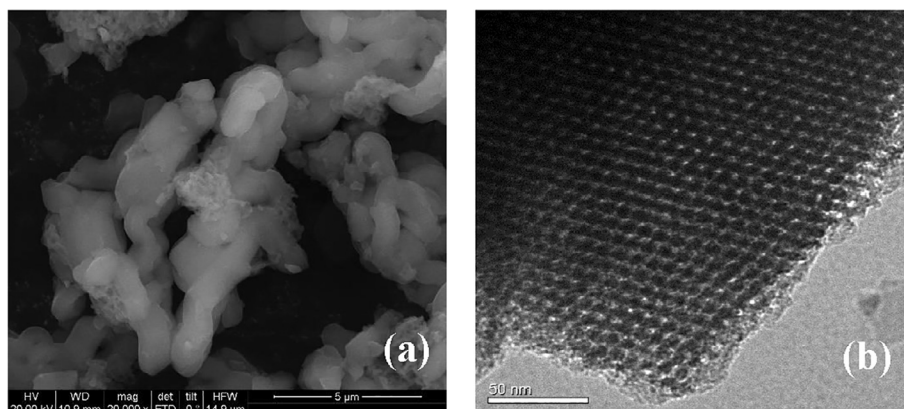
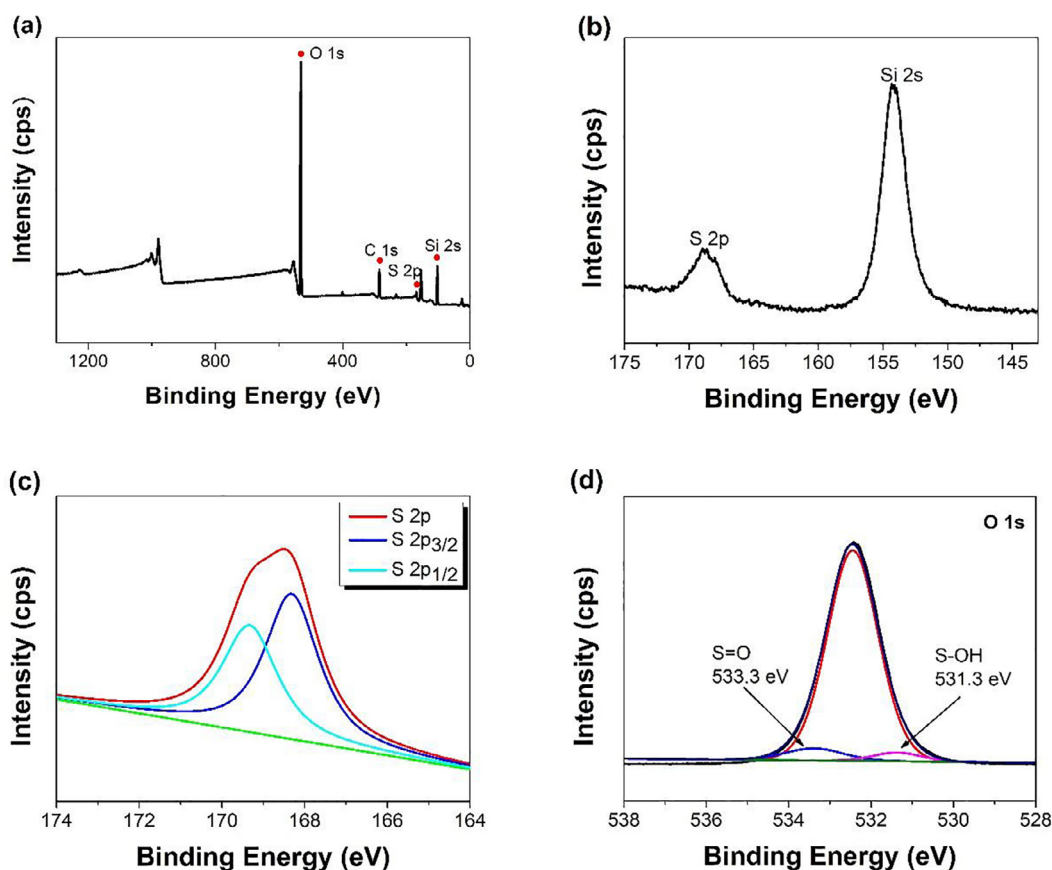
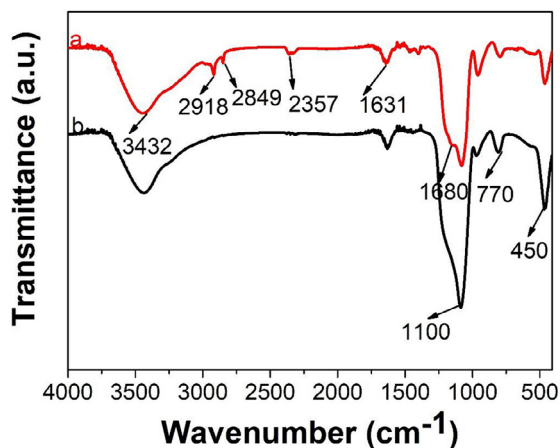
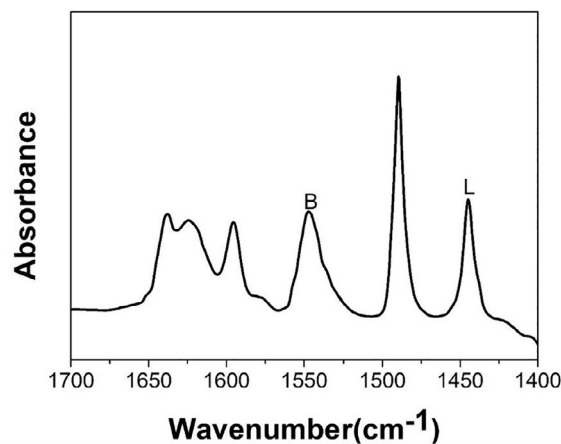


Fig. 3. Scanning electron microscopy images (a) and transmission electron microscopy images (b) of SBA-15- SO_3H .

Fig. 4. XPS profiles of SBA-15-SO₃H.Fig. 5. FT-IR spectra of samples: (a) SBA-15; (b) SBA-15-SO₃H.Fig. 6. Py-FITIR spectrum of SBA-15-SO₃H.

15-SO₃H. As seen in Fig. 4c, the S 2p photoelectron peaks centred at 168.36 and 169.33 eV are attributed to the binding energies of S 2p_{3/2} and S 2p_{1/2}, respectively, which are typical of -SO₃H. The results indicate the complete oxidation of the mercapto groups to sulphonic groups [32]. In the O 1s spectrum, due to the chemical states of oxygen in H₂SO₄ and -SO₃H, there are peaks of the S-OH bonds and S-O bonds located at 531.3 and 533.3 eV, respectively [33]. Therefore, we could infer by the presence of oxygen and sulphur that sulphonic acid groups were successfully attached to the surface of SBA-15-SO₃H [34].

FT-IR spectroscopy, plotted in Fig. 5, further evidences that the organosulphonic acid groups are added into the mesoporous structure of SBA-15. In the FT-IR spectrum, three peaks at 1100, 770 and 450 cm⁻¹ belong to the vibrations of Si-O-Si bond, which correspond to

the condensed silica network's asymmetric stretching, symmetric stretching and bending vibration, respectively [29]. Compared with SBA-15, the SBA-15-SO₃H has new IR absorption bands at 2918 and 2849 cm⁻¹, which could be reasonably assigned to the methylene C-H stretching vibration of propyl groups [29]. The IR band at 2575 cm⁻¹ was presumably due to the S-H stretching vibration. However, in Fig. 5b, the band has disappeared, due to the formation of -SO₃H groups after oxidation with H₂O₂ [34]. The bands at 3432 cm⁻¹ and 1631 cm⁻¹ can be assigned to S-OH stretching vibration. In addition, O=S=O asymmetric and symmetric stretching vibrations of -SO₃H groups appeared at 1080 cm⁻¹ and 1065 cm⁻¹, which indicates the existence of sulphonic acid groups in the SBA-15-SO₃H. In all, the organosulphonic groups have been successfully added into the SBA-15

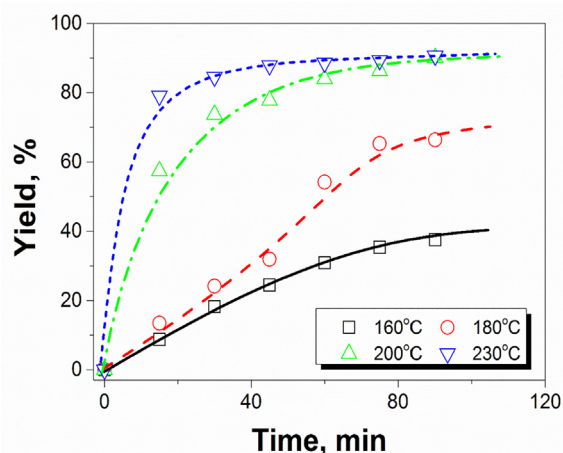


Fig. 7. Ethyl ester yield as a function of reaction temperature and time on SBA-15-SO₃H.

support to produce the SBA-15-SO₃H catalyst.

To elucidate the acid sites in the SBA-15-SO₃H, we used the FTIR spectrum of adsorbed pyridine. It can be seen from Fig. 6 that the infrared absorption at 1450 cm⁻¹ is attributed to pyridine adsorption on the Lewis acid sites, while the infrared absorption at 1545 cm⁻¹ belongs to the Brønsted acid sites that were mainly due to the -SO₃H groups [35]. There are infrared absorption peaks at 1455 and 1546 cm⁻¹, which illustrate that the sample has Lewis and Brønsted acid sites [36]. Moreover, the acidity of the sulphonic acid-functionalized SBA-15 was determined by acid-base titration. A 0.05 g sample was dispersed in 30 g NaCl (10 wt%) solution, stirred at room temperature for 24 h, and then filtered. The filtrate was titrated with 0.05 mol L⁻¹ NaOH solution, and the acid amount was found to be 1.95 mmol/g for SBA-15-SO₃H, whereas blank SBA-15 had no acid amount. When we performed the reaction for 60 min at a temperature of 200 °C with 5.0 wt% catalyst, the conversion yield of triglyceride

with SBA-15 was 4.7%, while that with SBA-15-SO₃H reached 88.1%. Therefore, the acid strength of the SO₃H groups plays a vital role in catalysis.

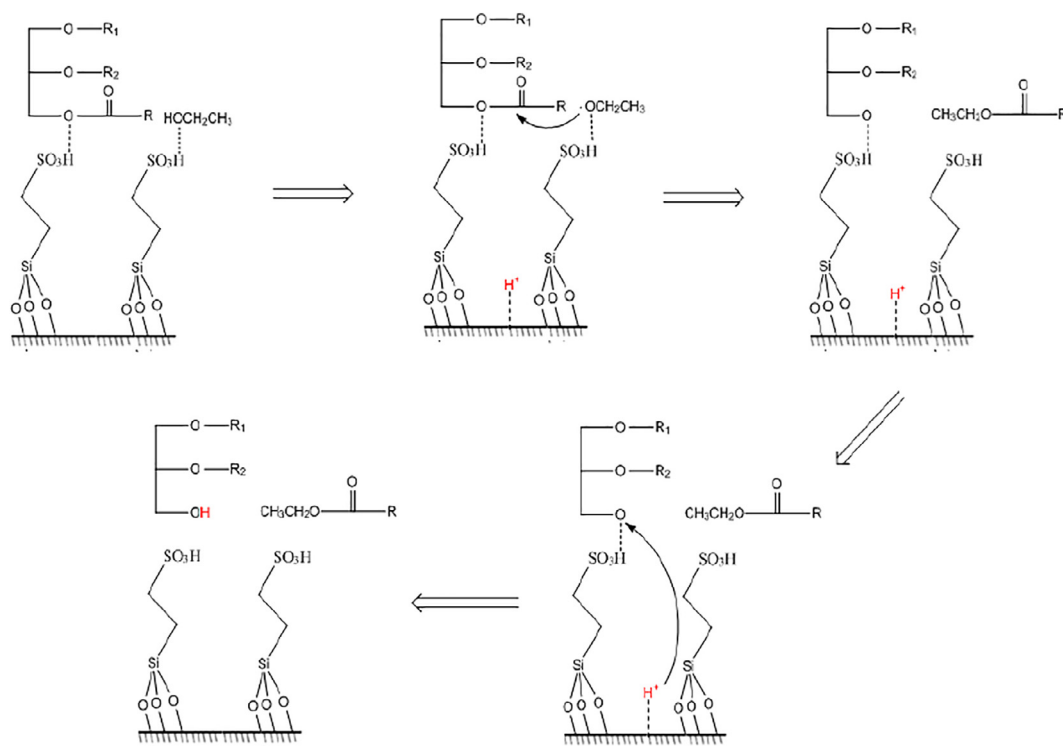
3.3. Transesterification of trilaurin by SBA-15-SO₃H

We further evaluated the effects of the sulphonated modified SBA-15 catalyst on the efficiency of the transesterification of triglyceride. The experiments were conducted using different temperatures and times as parameters. The detailed reaction conditions were a triglyceride mole ratio of 1:10 with ethanol, 5.0 wt% loading for the SBA-15-SO₃H catalyst, reaction temperatures of 160, 180, 200 or 230 °C, and reaction times of 15, 30, 60, 75 or 90 min.

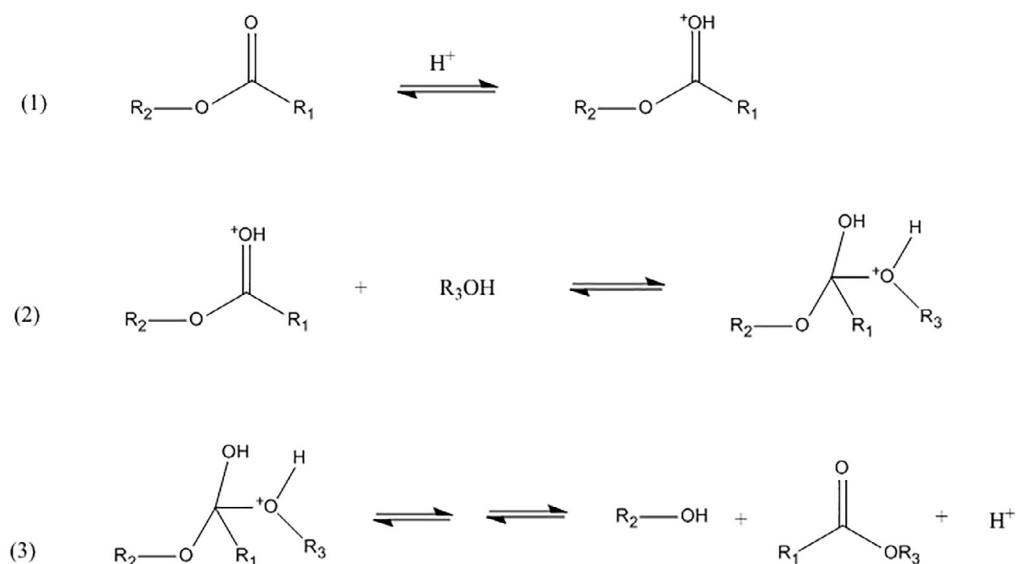
In Fig. 7, we observed an approximately 90% yield of ethyl esters at 200 and 230 °C within 90 min. At the lower temperatures, however, the ethyl ester yield was very low, with a maximum of approximately 6.5%. At the same reaction time, with the increase in temperature, the yield of ethyl ester steadily increased. Certainly, the longer time and higher temperature benefit the transesterification of triglyceride.

Guan et al. reported the kinetics of the trilaurin transesterification to ethyl esters, in which the products include ethyl esters (EE), unethyl esterified compounds (uEE) and glycerin (GL) [17]. Our experimental results illustrate that a large amount of EE and uEE were produced; the primary products were EE, with over 90% of the total yield, and the others were uEE.

Furuta et al. [7] compared the conversions of transesterification with solid superacid catalysis of SO₄²⁻/SnO₂ (STO), tungstated zirconia-alumina (WZA) and sulphated zirconia-alumina (SZA), finding conversions of only 10%, 47% and 26% at 200 °C, respectively. To reach 90% conversion, a high reaction temperature (250 °C) and long reaction time (20 h) were required by the tungstated zirconia-alumina (WZA) [37]. Jacobson et al. [38] reported low ester yields (65%) at 10 h and 200 °C over WO₃ on ZrO₂-Al₂O₃. Additionally, SO₄²⁻/ZrO₂ provided the highest yield of methyl esters, 90.3%, at 4 h and 200 °C [39]. Another study showed that SO₄²⁻/ZrO₂ only achieved a yield of 85% at 230 °C [37]. One of the solid zeolite catalysts was also applied to



Scheme 1. The mechanism of the catalytic transesterification by SBA-15-SO₃H.



Scheme 2. Homogeneous base-catalysed reaction mechanism for the transesterification.

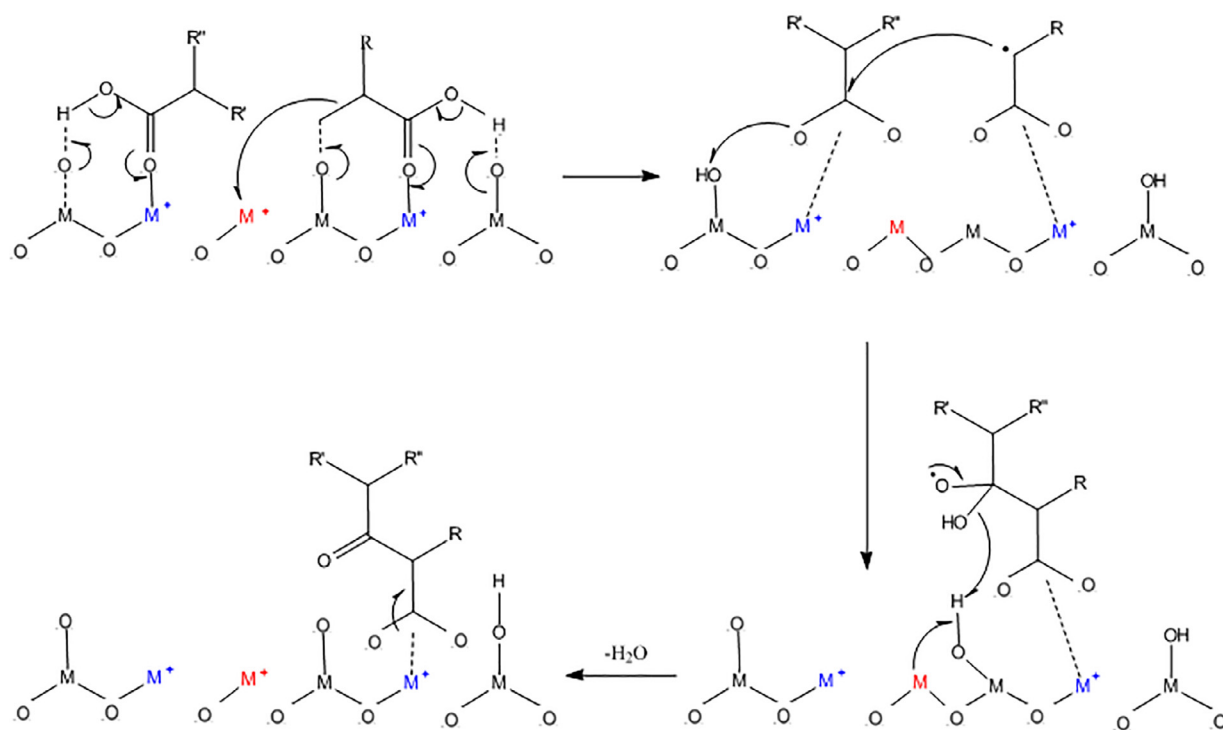
the transesterification, but the highest biodiesel yield attained was only 26.6% at a rather high reaction temperature of 460 °C. Compared with those catalysts, SBA-15-SO₃H in our study presented a high yield in a short time and at a moderate temperature. Therefore, this catalyst is one of most effective acid catalysts for the transesterification process.

3.4. Mechanism

The reactions of transesterification of triglyceride over solid acid catalysts are different from the base catalysts, as shown in Scheme 1. We postulated that the most important processes are the abstraction of

hydrogens from alcohols and α -substituted carboxylic glyceride. The following section will give a detailed discussion about the mechanism.

The abstraction of hydrogen from alcohols is the essential process for the transesterification of triglyceride. Pham et al. [40] gave an insight review about the ketonization of carboxylic acids over solid acids, which is somewhat similar to the transesterification of triglyceride. Ketonization (or ketonic decarboxylation) is a reaction that converts two carboxylic acid molecules into a ketone, carbon dioxide, and water, which has been well studied since 1858. The process proposes the requirement for an α -hydrogen in at least one of the carboxylic acids participating in the reaction, which has been well documented. The α -



Scheme 3. Proposed β -ketoacid-based mechanism for the ketonization of carboxylic acid.

hydrogen is defined as the hydrogen atom bonded to a carbon atom in the α position relative to a carbonyl group. Similarly, we also proposed the abstraction of hydrogen from alcohol onto the surface, which can enhance the nucleophilicity of alcohols.

There would be some disputes about which O atom of the triglyceride would be attacked by the acidic surface. One potential pathway is that the O atom of the carboxyl group would be protonated by the acid catalyst surface, rather than the α position, i.e., the oxygen atom on the C–O–C [41]. This pathway will be similar to a homogeneous acid-catalysed reaction mechanism for the transesterification of triglycerides proposed by Lotero, Liu, Lopez, Suwannakarn, Bruce and Goodwin [42]. This mechanism involves protonation of the carbonyl group by the acid catalyst and then nucleophilic attack of the alcohol, forming a tetrahedral intermediate, followed by proton migration and breakdown of the intermediate, as shown in Scheme 2. The mechanism is similar to the β -ketoacid intermediate mechanism for the ketonization of carboxylic acid. This mechanism is shown in Scheme 3, where M represents a metal. Proton migration and breakdown of the intermediate tend to form H₂O as an intermediate [43]. However, we did not observe the formation of water during the process.

Thus, we prefer α -substituted carboxylic glyceride as the main mechanism. The oxygen atom on the C–O–C provides a pair of electrons for the –SO₃H. The attack to the oxygen atom will result in a weakened C–O–C bond to produce the carbonyl carbon –OR1. Then, the nucleophilic attack of the alcohol leads to the α -substituted carboxylic glyceride. Finally, monoglycerides, diglycerides or glycerine are released from the surface by the proton (H⁺) replacement, as shown in Scheme 1.

4. Conclusions

In the work, we compared various catalysts. The conversion yield of triglyceride reached 90.1% and was maintained for 90 min at 200 °C with 5.0 wt% SBA-15-SO₃H. The results showed that more highly acidic catalysts and higher surface areas lead to higher catalytic activity. The mechanism indicates that the most important processes are the abstraction of hydrogen atoms from alcohols and α -substituted carboxylic glyceride. In the initial transesterification, the hydrogen atom of the alcohol can be attracted to the surface. Then, the nucleophilic attack of the alcohol leads to the α -substituted carboxylic glyceride. At last, monoglycerides, diglycerides or glycerine are released from the surface by proton (H⁺) replacement.

Acknowledgements

This work is supported by the National Natural Science Foundation of China (21767015) and National Key R&D Program of China (2017YFC0210504), Collaborative Innovation Centre of Western Typical Industry Environmental Pollution Control.

Appendix A. Supplementary data

Supplementary data associated with this article can be found, in the online version, at <https://doi.org/10.1016/j.ica.2018.07.032>.

References

- G.W. Huber, A. Sara Iborra, A. Corma, Synthesis of transportation fuels from biomass: chemistry, catalysts, and engineering, *Chem. Rev.* (2006) 4044–4098.
- A.J. Ragauskas, C.K. Williams, B.H. Davison, G. Britovsek, J. Cairney, C.A. Eckert, F.W. Jr, J.P. Hallett, C.L. Liotta, The path forward for biofuels and biomaterials, *Science* 311 (2006) 484–489.
- J. Calero, G. Cumplido, D. Luna, E.D. Sancho, C. Luna, A. Posadillo, F.M. Bautista, A.A. Romero, C. Verduogoscamilia, Production of a biofuel that keeps the glycerol as a monoglyceride by using supported KF as heterogeneous catalyst, *Energies* 7 (2014) 3764–3780.
- L. Lin, H. Cui, V. Saritporn, Z. Xiao, W. Wu, A. Zhang, M. Wael, C. Li, Synthesis of recyclable hollow Fe/C-SO₃H fiber as a catalyst for the production of biodiesel, *Environ. Prog. Sustain. Energy* 33 (2014) 1432–1437.
- A. Brito, M.E. Borges, N. Otero, Zeolite Y as a Heterogeneous Catalyst in Biodiesel Fuel Production from Used Vegetable Oil, *Energy Fuels* 21 (2007) 3280–3283.
- D. Royon, M. Daz, G. Ellenrieder, S. Locatelli, Enzymatic production of biodiesel from cotton seed oil using t-butanol as a solvent, *Bioresour. Technol.* 98 (2007) 648–653.
- S. Furuta, H. Matsuhashi, K. Arata, Biodiesel fuel production with solid superacid catalysis in fixed bed reactor under atmospheric pressure, *Catal. Commun.* 5 (2004) 721–723.
- C.S. Macleod, A.P. Harvey, A.F. Lee, K. Wilson, Evaluation of the activity and stability of alkali-doped metal oxide catalysts for application to an intensified method of biodiesel production, *Chem. Eng. J.* 135 (2008) 63–70.
- A.E. Ghaly, D. Dave, M.S. Brooks, S. Budge, Production of biodiesel by enzymatic transesterification: review, *Am. J. Biochem. Biotechnol.* 6 (2010) 54–76.
- R.W.M. Mounguengui, C. Brunschwig, B. Baré, P. Villeneuve, J. Blin, Are plant lipases a promising alternative to catalyze transesterification for biodiesel production? *Prog. Energy Combust. Sci.* 39 (2013) 441–456.
- X. Lei, W. Lu, Q. Peng, H. Li, T. Chen, S. Xu, F. Zhang, Activated MgAl-layered double hydroxide as solid base catalysts for the conversion of fatty acid methyl esters to monoethanolamides, *Appl. Catal. A* 399 (2011) 87–92.
- Y.S. Lu, Z.W. Zhang, Y.F. Xu, Q. Liu, G.R. Qian, Cefael mixed oxide derived heterogeneous catalysts for transesterification of soybean oil to biodiesel, *Bioresour. Technol.* 190 (2015) 438–441.
- Y.B. Huang, T. Yang, M.C. Zhou, H. Pan, Y. Fu, Microwave-assisted alcoholysis of furfural alcohol into alkyl levulinates catalyzed by metal salts, *Green Chem.* 18 (2016) 1516–1523.
- J. Nowicki, J. Lach, M. Organek, E. Sabura, Transesterification of rapeseed oil to biodiesel over Zr-doped MgAl hydrotalcites, *Appl. Catal. A* 524 (2016) 17–24.
- J.A. Cecilia, C. García-Sancho, J.M. Mérida-Robles, J. Santamaría-González, R. Moreno-Tost, P. Maireles-Torres, V and V-P containing Zr-SBA-15 catalysts for dehydration of glycerol to acrolein, *Catal. Today* 254 (2015) 43–52.
- Q.Q. Guan, S. Hua, L. Jing, J.J. Gu, B. Li, R.R. Miao, Q.L. Chen, N. Ping, Biodiesel from transesterification at low temperature by AlCl₃ catalysis in ethanol and carbon dioxide as cosolvent: process, mechanism and application, *Appl. Energy* 164 (2016) 380–386.
- Q. Guan, Y. Li, Y. Chen, Y. Shi, J. Gu, B. Li, R. Miao, Q. Chen, P. Ning, Sulfonated multi-walled carbon nanotubes for biodiesel production through triglycerides transesterification, *RSC Adv.* 7 (2017) 7250–7258.
- H. Veisi, A. Sedrpoushan, A.R. Faraji, M. Heydari, S. Hemmati, B. Fatahi, A mesoporous SBA-15 silica catalyst functionalized with phenylsulfonic acid groups (SBA-15-Ph-SO₃H) as a novel hydrophobic nanoreactor solid acid catalyst for a one-pot three-component synthesis of 2H-indazolo[2,1-b]phthalazine-triones and triazolo [1,2-a]indazole-triones, *RSC Adv.* 5 (2015) 68523–68530.
- Y. Li, S. Zhao, Q. Hu, Z. Gao, Y. Liu, J. Zhang, Y. Qin, Highly efficient CoOx/SBA-15 catalysts prepared by atomic layer deposition for the epoxidation reaction of styrene, *Catal. Sci. Technol.* 7 (2017) 2032–2038.
- Y.Q. Zhang, S.J. Wang, J.W. Wang, L.L. Lou, C. Zhang, S. Liu, Synthesis and characterization of Zr-SBA-15 supported tungsten oxide as a new mesoporous solid acid, *Solid State Sci.* 11 (2009) 1412–1418.
- T. Ma, Z. Yun, W. Xu, L. Chen, L. Li, J. Ding, R. Shao, Pd-H₃PW₁₂O₄₀/Zr-MCM-41: an efficient catalyst for the sustainable dehydration of glycerol to acrolein, *Chem. Eng. J.* 294 (2016) 343–352.
- E.I. Ross-Medgaarden, W.V. Knowles, T. Kim, M.S. Wong, W. Zhou, C.J. Kiely, I.E. Wachs, New insights into the nature of the acidic catalytic active sites present in ZrO₂-supported tungsten oxide catalysts, *J. Catal.* 256 (2008) 108–125.
- F. Liu, C. Liu, W. Kong, C. Qi, A. Zheng, S. Dai, Design and synthesis of micro-mesoporous polymers with versatile active sites and excellent activities in the production of biofuels and fine chemicals, *Green Chem.* 18 (2016) 6536–6544.
- Y. Gu, A. Azzouzi, Y. Pouilloux, F. Jerome, J. Barrault, Heterogeneously catalyzed etherification of glycerol: new pathways for transformation of glycerol to more valuable chemicals, *Green Chem.* 10 (2008) 164–167.
- G.M. Ziarani, A. Badiel, N.H. Mohtasham, N. Lashgari, Sulfonic acid functionalized nanoporous silica (SBA-Pr-SO₃H) as an efficient catalyst for the one-pot synthesis of 2h-indazolo[1,2-B] phthalazine-triones, *J. Chil. Chem. Soc.* 59 (2014) 2271–2274.
- W. Zhu, S. Ge, Q. Shao, Adsorption properties of ZrO₂ hollow microboxes prepared using CaCO₃ cubes as templates, *RSC Adv.* 6 (2016) 81736–81743.
- W. He, J. Liu, Z. Cao, C. Li, Y. Gao, Preparation and characterization of mono-disperse zirconia spherical nanometer powder via lamellar liquid crystal template method, *Chin. J. Chem. Eng.* 23 (2015) 1721–1727.
- F. Alrouh, A. Karam, A. Alshaghel, S. El-Kadri, Direct esterification of olive-pomace oil using mesoporous silica supported sulfonic acids, *Arabian J. Chem.* 10 (2012) 281–286.
- W. Xie, C. Zhang, Propylsulfonic and arenesulfonic functionalized SBA-15 silica as an efficient and reusable catalyst for the acidolysis of soybean oil with medium-chain fatty acids, *Food Chem.* 211 (2016) 74–82.
- F.X. Zhu, H.X. Li, In situ preparation of Au-SH@SO₃H-SBA-15 catalyst with enhanced activity and durability in alkyne hydration, *Chin. J. Chem.* 32 (2014) 1072–1076.
- F. Zhou, J. Tang, Z. Fei, X. Zhou, X. Chen, M. Cui, X. Qiao, Efficient cyclohexyl acrylate production by direct addition of acrylic acid and cyclohexene over SBA-15-SO₃H, *J. Porous Mater.* 21 (2014) 149–155.
- M.L. Testa, V. La Parola, A.M. Venezia, Transesterification of short chain esters using sulfonic acid-functionalized hybrid silicas: Effect of silica morphology, *Catal. Today* 223 (2014) 115–121.
- Y. Wei, X. Ling, L. Zou, D. Lai, H. Lu, Y. Xu, A facile approach toward preparation of sulfonated multi-walled carbon nanotubes and their dispersibility in various

- solvents, *Colloids Surf. A* 482 (2015) 507–513.
- [34] H. Yu, Y. Jin, Z. Li, F. Peng, H. Wang, Synthesis and characterization of sulfonated single-walled carbon nanotubes and their performance as solid acid catalyst, *J. Solid State Chem.* 181 (2008) 432–438.
- [35] F. Zhou, J. Tang, Z. Fei, X. Zhou, X. Chen, M. Cui, X. Qiao, Efficient cyclohexyl acrylate production by direct addition of acrylic acid and cyclohexene over SBA-15-SO₃H, *J. Porous Mater.* 21 (2013) 149–155.
- [36] G.C.A.J.A. Dumesic, Acidic properties of binary oxide catalysts: I. Mössbauer spectroscopy and pyridine adsorption for iron supported on silica, *J. Catal.* 101 (1986) 103–113.
- [37] M.K. Lam, K.T. Lee, A.R. Mohamed, Homogeneous, heterogeneous and enzymatic catalysis for transesterification of high free fatty acid oil (waste cooking oil) to biodiesel: a review, *Biotechnol. Adv.* 28 (2010) 500–518.
- [38] K. Jacobson, R. Gopinath, L. Meher, A. Dalai, Solid acid catalyzed biodiesel production from waste cooking oil, *Appl. Catal. B* 85 (2008) 86–91.
- [39] J. Jitputti, B. Kitiyanan, P. Rangsunvigit, K. Bunyakiat, L. Attanatho, P. Jenvanitpanjakul, Transesterification of crude palm kernel oil and crude coconut oil by different solid catalysts, *Chem. Eng. J.* 116 (2006) 61–66.
- [40] T.N. Pham, T. Sooknoi, S.P. Crossley, D.E. Resasco, Ketonization of carboxylic acids: mechanisms, catalysts, and implications for biomass conversion, *ACS Catal.* 3 (2013) 2456–2473.
- [41] A. Talebian-Kiakalaieh, N.A.S. Amin, H. Mazaheri, A review on novel processes of biodiesel production from waste cooking oil, *Appl. Energy* 104 (2013) 683–710.
- [42] E. Lotero, Y.J. Liu, D.E. Lopez, K. Suwannakarn, D.A. Bruce, J.G. Goodwin, Synthesis of biodiesel via acid catalysis, *Indus. Eng. Chem. Res.* 44 (2005) 5353–5363.
- [43] O. Nagashima, S. Sato, R. Takahashi, T. Sodesawa, Ketonization of carboxylic acids over CeO₂-based composite oxides, *J. Mol. Catal. A Chem.* 227 (2005) 231–239.